Journal of Digital Imaging

Comparison of Algorithms to Enhance Spicules of Spiculated Masses on Mammography

Mehul P. Sampat,[1] Gary J. Whitman,[2] Alan C. Bovik,[3] and Mia K. Markey[1]

We have developed an algorithm for enhancement of spicules of spiculated masses, which uses the discrete radon transform. Previously, we employed a commonly used method to compute the discrete radon transform, which we refer to as the DRT. Recently, a new, more exact method to compute the discrete radon transform was developed by Averbuch et al, which is called the fast slant stack (FSS) method. Our hypothesis was that this new formulation would help to improve our enhancement algorithm. To test this idea, we conducted multiple two-alternative-forced-choice observer studies and found that most observers preferred the enhanced images generated with the FSS method.

KEY WORDS: Image processing, image enhancement, breast, computer-aided diagnosis (CAD), algorithms, mammography CAD

INTRODUCTION

Background

The American Cancer Society estimates that 212,920 women will be diagnosed with breast cancer and 40,970 women will die of the disease in the United States in 2006.[1] Screening mammography, x-ray imaging of the breast, is currently the most effective tool for early detection of breast cancer. Radiologists visually search mammograms for specific abnormalities. Some of the important signs of breast cancer that radiologists look for are clusters of microcalcifications, masses, and architectural distortions. Spiculated masses are characterized by radiating lines or spicules from a central mass of tissue. Spiculated masses carry a much higher risk of malignancy than calcifications or other types of masses.[2]

Detection of suspicious abnormalities on mammography is a repetitive and fatiguing task. For every thousand cases analyzed by a radiologist, only three to four are cancerous, and thus, an abnormality may be overlooked. Computer-aided detection (CADe) systems have been developed to aid radiologists in detecting mammographic lesions that may indicate the presence of breast cancer.[3] These systems act only as a second reader and the final decision is made by the radiologist. Some studies have shown that CADe systems, when used as an aid, have improved radiologists' accuracy for detecting breast cancer.[4–7]

However, current CADe systems are dramatically better at detecting microcalcifications than spiculated masses. The most widely used commercial CADe system is reported to have 98.5% sensitivity at 0.185 false positives per image (FPI) for microcalcification clusters but only 86% sensitivity at 0.24 FPI for spiculated masses.[8] Calcifications have a simple biomorphology and it

[1]*From the Department of Biomedical Engineering, ENS 610 The University of Texas at Austin, 1 University Station C0800, Austin, Texas 78712-1084, USA.*

[2]*From the Division of Diagnostic Imaging, The University of Texas M. D. Anderson Cancer Center, Houston, Texas 77030, USA.*

[3]*From the Department of Electrical and Computer Engineering, The University of Texas at Austin, Austin, Texas 78712, USA.*

Correspondence to: Mehul P. Sampat, PhD, Department of Biomedical Engineering, ENS 610 The University of Texas at Austin, 1 University Station C0800, Austin, Texas 78712-1084, USA; tel: +1-512-2936090; fax: +1-512-4710616; e-mail: mehul.sampat@ieee.org

Copyright © 2007 by Society for Imaging Informatics in Medicine

doi: 10.1007/s10278-007-9015-x

is easy to model them. In comparison, spiculated masses exhibit great variability in their shapes and dimensional attributes (Fig. 1).

Overview of our CADe Algorithm

We have developed a new evidence-based algorithm for CADe of spiculated lesions.[9] By evidence-based, we mean that we use the statistics of the physical characteristics of spiculated lesions to determine the parameters of the detection algorithm. Our algorithm consists of two steps, an enhancement step followed by a filtering step. In the first step, spicules are enhanced using a new technique in which a linear filter is applied to the discrete radon transform (DRT) of the image. In the second step, the enhanced images are filtered with a new class of linear image filters called radial spiculation filters. We have invented these filters specifically for detecting spiculated lesions that are marked by converging lines or spiculations.

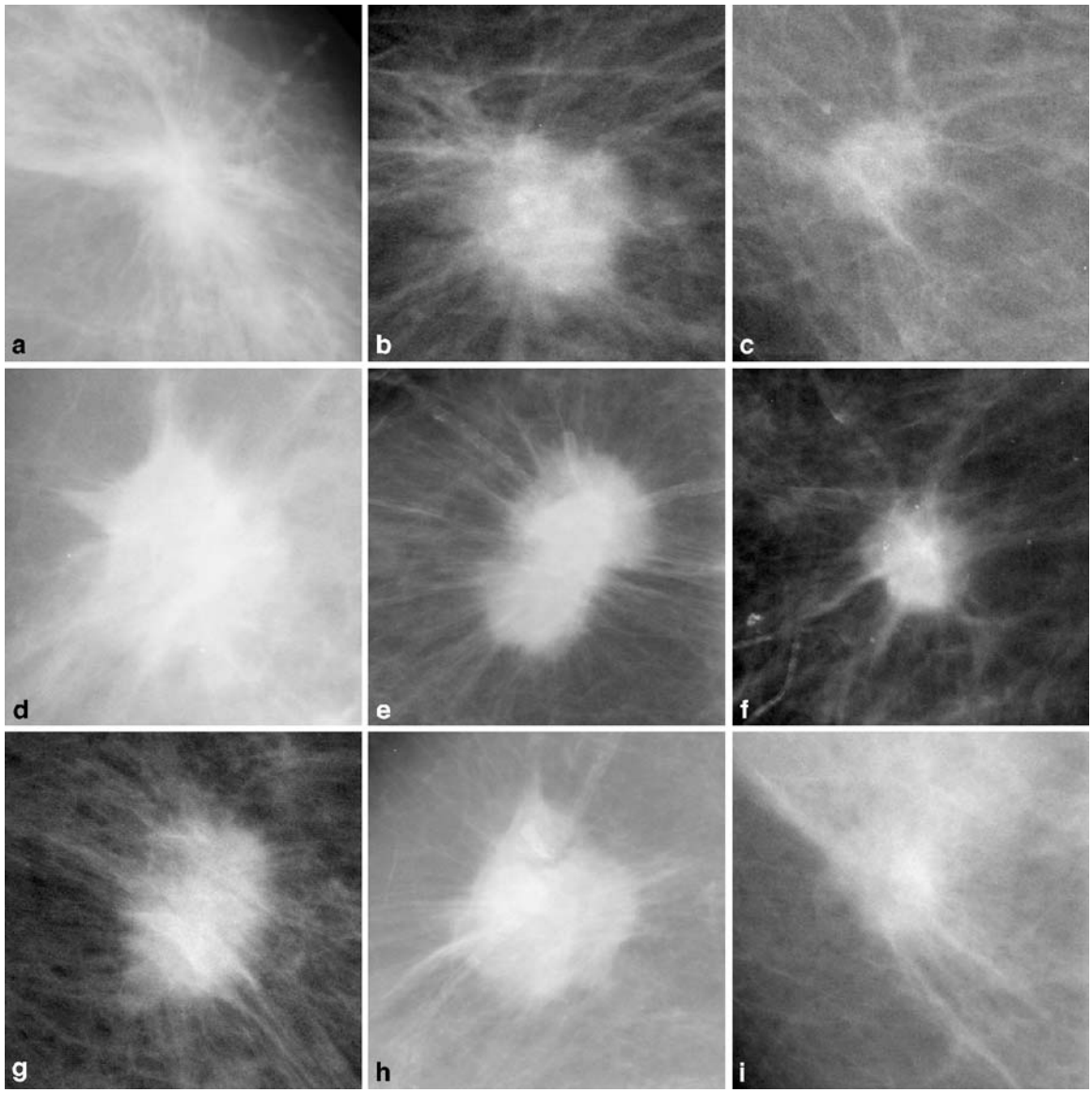

Fig 1. Examples of spiculated masses. We can see that there is a great variability in the appearance of spiculated masses on mammography.

A key aspect of this work is that all parameters of the CADe algorithm are based on the physical measurements of the properties of spiculated lesions. We have established that parameters of spicules (e.g., spicule width and length) can be reliably measured by experienced radiologists,[10] and we have collected a small database of such measurements for setting the parameters of the detection algorithm.

Overview of This Paper

One component of our CADe algorithm is a new method for the enhancement of spicules on spiculated lesions (Fig. 2). In this method, we compute a discrete form of the radon transform of a mammogram and apply a filter in the radon domain. The enhanced image is obtained by computing the inverse radon transform. The most common approach to computing a DRT is based on computing the projection of the image intensities along radial lines oriented at specific angles; for the rest of this paper, we refer to this traditional formulation as the DRT. Recently, the fast slant stack (FSS) method[20] was developed to compute a discrete form of the radon transform of an image. This algorithm is one-to-one and is invertible on its range, and it is computationally efficient. In this work, we compare the effect of using the DRT approach to discretizing the radon transform versus the new FSS algorithm in our spicule-enhancement strategy. In this study we used regions of interest containing spiculated lesions (as opposed to full mammograms) to ensure that the observers were not distracted by other structures in the mammogram.

MATERIALS AND METHODS

Continuous Radon Transform

In this section, we describe the continuous radon transform and compare some of the approaches to discretizing it. The continuous radon transform, $g(\rho\theta)$, of an image [represented by the function $f(x,y)$] can be viewed as a series of line integrals through the image.[11] Mathematically, this is given by the following:

$$g(\rho,\theta) = \int_{y=-\infty}^{y=+\infty}\int_{x=-\infty}^{x=+\infty} f(x,y)\delta(\rho - x\cos(\theta) - y\sin(\theta))\cdot dx\cdot dy$$

A number of researchers have focused on developing DRTs and inverse radon transforms (reconstructing images from the projections). A discrete version of the radon transform can be computed in a number of ways. These include summing image intensities for each line through the image,[12] by using Fourier-based techniques,[13] and by using a multiscale approach.[14]

Methods for computing an inverse radon transform have received more attention in medical imaging because the projection data obtained from several important modalities (e.g., computed tomography, positron emission tomography) are the coefficients of the radon transform of the image. Both analytical methods (e.g., filtered back projection) and iterative methods, which can be algebraic or statistical methods,[15–18] have been developed for inverting the radon transform and reconstructing the image.

Description of the Different Forms of the DRTs Used

In this work we have compared the performance of a commonly used formulation of a DRT, the DRT method, with a new formulation of the DRT, called the FSS method.[20] In the DRT formulation, the DRT is obtained by computing the projection of the image intensities along radial lines oriented at specific angles. Each projection is obtained by summing the image intensity values along a specific angle. The inverse radon transform is computed by using the filtered back

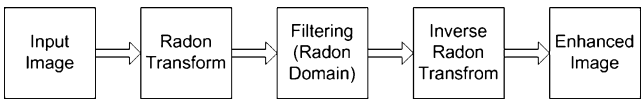

Fig 2. The steps of our enhancement algorithm. The radon transform of the image is first computed and the columns of the radon domain are filtered with a column filter. The enhanced image is obtained by computing the inverse radon transform.

projection algorithm. The details of this method can be found in the work by Bracewell.[12]

In the FSS method, the radon domain data are computed using the projection-slice theorem. This theorem states that the Fourier transform of the radon transform coefficients from a projection of an image at a fixed angle is equivalent to a slice of the 2-dimensional Fourier transform of the image. Thus, to compute the radon transform one needs the Fourier transform values in a non-Cartesian grid. This grid is referred to as a pseudopolar grid and the pseudopolar Fourier transform is computed on a non-Cartesian grid using a chirp-Z transform. The inverse radon transform is computed iteratively using a conjugate gradient solver. The details of this method can be found in the article by .[20] Averbuch et al state that the FSS method algorithm is one-to-one, exact, and invertible on its range.[20]

Brief Review of Radon-based Approach to Enhance Spicules

In this section, we describe the intuition behind our radon-based approach to enhancing spicules. For clarity, we describe the method using the DRT formulation of the DRT[12] but note that this approach is applicable to any formulation of the DRT. Let $f(x,y)$ be an N-by-N image. Let the DRT be represented by $\hat{g}(\rho,\theta)$, which is defined as:

$$\hat{g}(\rho,\theta)=\sum_{y=-N/2}^{N/2}\sum_{x=-N/2}^{N/2} f(x,y)\delta(\rho-x\cos(\theta)-y\sin(\theta))$$

where $\delta(r)$ is the Kronecker impulse function, which is zero everywhere except when $r=0$. Hence, the term $\delta(\rho-x\cos(\theta)-y\sin(\theta))$ contributes summed values of $f(x,y)$ only along the line $\rho-x\cos(\theta)-y\sin(\theta)$, and thus, the value of $\hat{g}(\rho,\theta)$ for any (ρ,θ) is the sum of values of $f(x,y)$ along this line. Figure 3a provides a schematic explanation of the parameters of the radon domain.

An important property of the radon transform is that a line in the image space $f(x,y)$ maps to a unique peak in the radon domain (Fig. 3b, c). In addition, lines of different thickness have different representations in the radon domain. Figure 4 shows two lines of different thickness and their corresponding radon transforms. A single-pixel-thick line would be represented by a point in the radon domain,

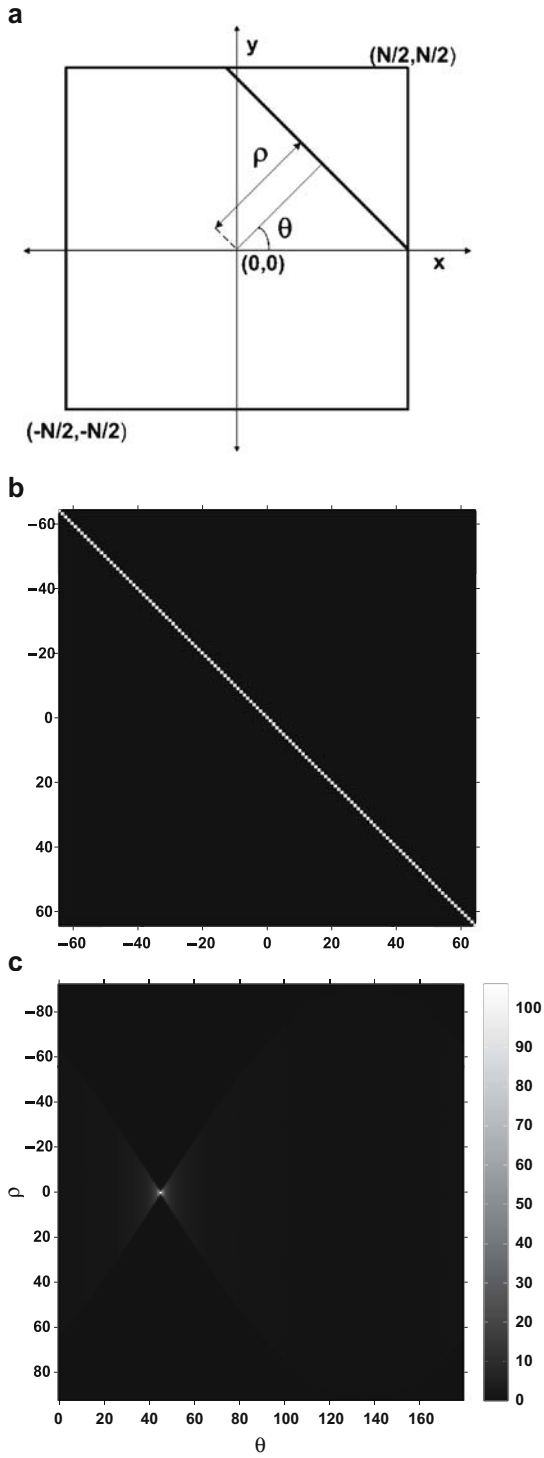

Fig 3. A schematic explanation of the radon transform. Each line in an image is uniquely defined by the parameters ρ and θ. To compute the radon transform, the image intensities are summed for every line in the image. One example of an image and its radon transform is shown in b and c.

whereas a four-pixel-thick line would be represented by four points along a column in the radon domain. Thus, by detecting "local peaks" along the columns in the radon domain, it is possible to detect the corresponding lines in the image. To do so, a number of peak detection algorithms can be used. While many approaches might be taken to identify peaks, our approach is to simply filter the columns of the radon domain with an appropriate bivalued, one-dimensional, linear filter with an impulse response that is a rectangle of width agreeing with the maximum spicule width to be highlighted. As mentioned earlier, the filter parameters were based on the measurements from an observer study in which radiologists measured the properties of these lesions. This approach has the advantages of both directness and simplicity. Application of this simple filter to the radon domain, followed by an inverse radon transform, will yield an enhanced image with amplified linear structures (spicules) of the requisite widths, all other structures being suppressed. A detailed description of our algorithm can be obtained in a previous publication.[9] The goal of this work was to compare the effect of using the DRT formulation versus the FSS formulation of the digital radon transform in our spicule-enhancement algorithm.

Experimental Setup

The images for this study were obtained from the Digital Database for Screening Mammography, http://marathon.csee.usf.edu/Mammography/Database.html.[19] We selected 30 mediolateral oblique images, each containing a single spiculated mass. A region of interest containing the abnormality was cropped and used for all further analyses. The 30 images were enhanced using two versions of our spicule-enhancement algorithm. In the first version, the DRT formulation was used,

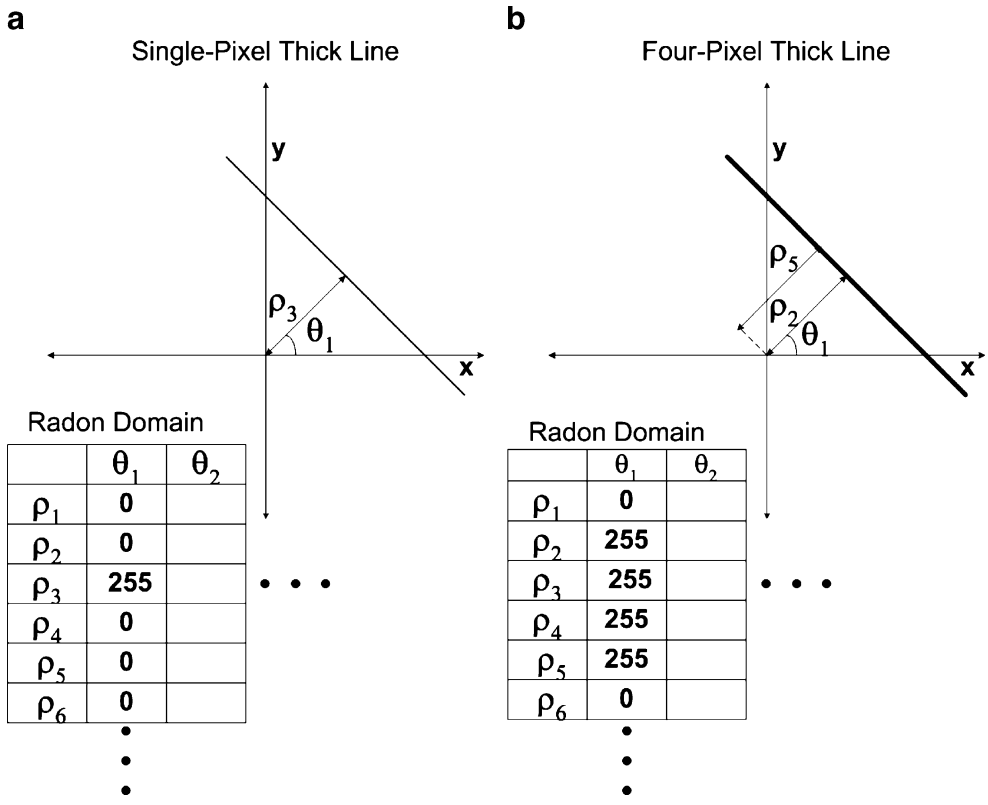

Fig 4. a A single-pixel-thick line *(left).* **b A four-pixel-thick line** *(right)* **and sections of their radon transforms. A** *line* **in an image maps to a peak of a particular width in the radon domain.**

whereas in the second version, the FSS formulation of the DRT was used.

To study the advantages of using the FSS formulation over the DRT formulation, we applied the following procedure. We conducted multiple two-alternative-forced-choice (2 AFC) observer studies. In the first study, the observer was a radiologist (GJW) with extensive expertise in breast imaging. In the second observer study, 10 engineering students from our research lab were selected as observers. For each image, the original image and the two enhanced images (obtained using the DRT and FSS formulations of the DRT) were shown to all of the observers and they were asked to choose the image in which the spicules were enhanced more prominently. We also measured the total time for obtaining 30 enhanced images using the DRT and FSS formulations. Both methods were implemented in MATLAB® (The MathWorks, Natick, MA, USA).

Figure 5 shows this experimental setup. Figure 5b shows the original image, Figure 5a shows the enhanced image obtained with the DRT-based method, and Figure 5c shows the enhanced image obtained with the FSS-based method. The positions of the enhanced images (left or right) were randomly selected so that the observers would not be able to tell by which method the enhanced image was generated.

RESULTS

The results of the 2 AFC observer study are presented in Table 1. For each observer, we counted the number of images for which he/she felt that the spicules were more apparent in the image enhanced with the FSS-based method as compared to the image enhanced with the DRT-based method. The radiologist preferred the enhanced images generated by the FSS-based method for 28 out of the 30 images (98.33%). Moreover, most of the engineering observers also preferred the images enhanced with the FSS-based method over those enhanced with the DRT-based method. On average, for 74.6% (standard deviation = 21.1%) of the images, all of 10 engineering observers felt that enhancement results of the FSS-based method were visually more appealing. There were only two images for which the radiologist, as well as most of the novice observers, preferred the enhanced image generated by the DRT-based method to that generated by the FSS-based method (Fig. 6). This was most likely due to the fact that the radiologist reported that he preferred images where edges were enhanced. He felt he could see more spicules in Figure 6c as compared to Figure 6a. In addition, he could see more detail in the region of the mass in Figure 6d as compared to Figure 6f. Similarly, three examples of images where most observers

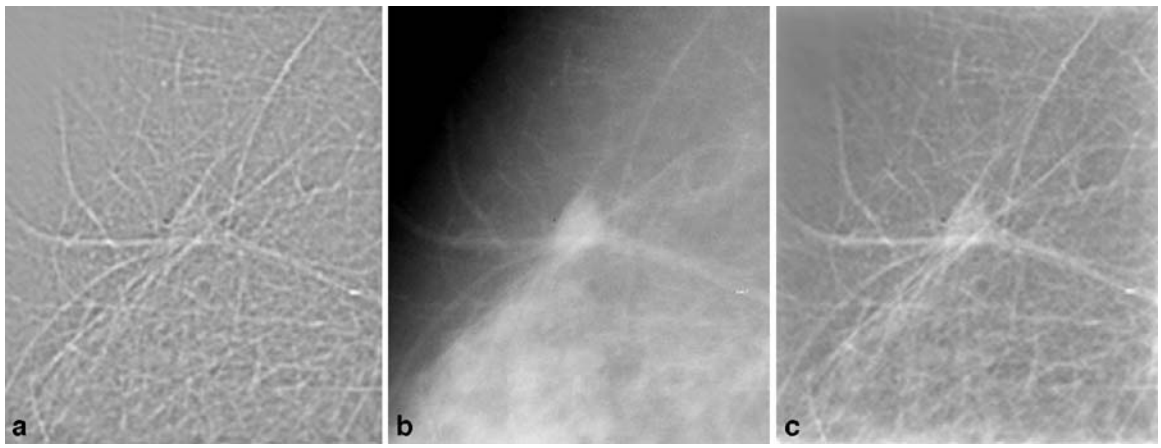

Fig 5. Screenshot of the observer experiments carried out. The *image in the center* is the original image and the *images on the left* and *right* are the enhanced images obtained with the DRT-based and FSS-based enhancement methods, respectively. The observer is asked to choose which enhanced image they found most visually appealing. For the 2-AFC observer studies experiments, the observers were not told from which method a particular enhanced image was generated and the images were shown in random order.

Table 1. Results of the 2-AFC Experiment

	% of Images for which the FSS-based Method was Rated as Superior
Observer 1	93 (28/30)
Observer 2	47 (14/30)
Observer 3	87 (26/30)
Observer 4	67 (20/30)
Observer 5	93 (28/30)
Observer 6	70 (21/30)
Observer 7	100 (30/30)
Observer 8	60 (18/30)
Observer 9	90 (27/30)
Observer 10	40 (12/30)

For each observer, the percentage of images where the observer felt the spicules were enhanced more prominently by the FSS-based method. On average, for 74% of images, the observers felt that the FSS-based method produced better enhancement results. Moreover, the radiologist preferred the images generated by the FSS-based method for 28 out of the 30 images (98%).

preferred the enhanced image generated by the FSS-based method are shown in Figure 7.

The FSS-based method was computationally more efficient than the DRT-based method. The total time required to run the DRT-based method on 30 images was 29.5 min, whereas the total time required for running the FSS-based method on 30 images was only 4.7 min. Thus, the FSS-based method was six times faster than the DRT-based method.

DISCUSSION

We have developed an algorithm for the CADe of spiculated masses, and an important component of this algorithm is a spicule-enhancement strategy. In this method, we compute the DRT of an image and apply a filter in the radon domain. In this work, we have compared the effects of using the DRT formulation versus the FSS formulation of the DRT in our spicule-enhancement algorithm.

This study showed that observers with and without experience in radiology found images enhanced by the FSS-based method to be more visually appealing. Moreover, the FSS-based formulation of the DRT was computationally more efficient than the commonly used DRT-based formulation.

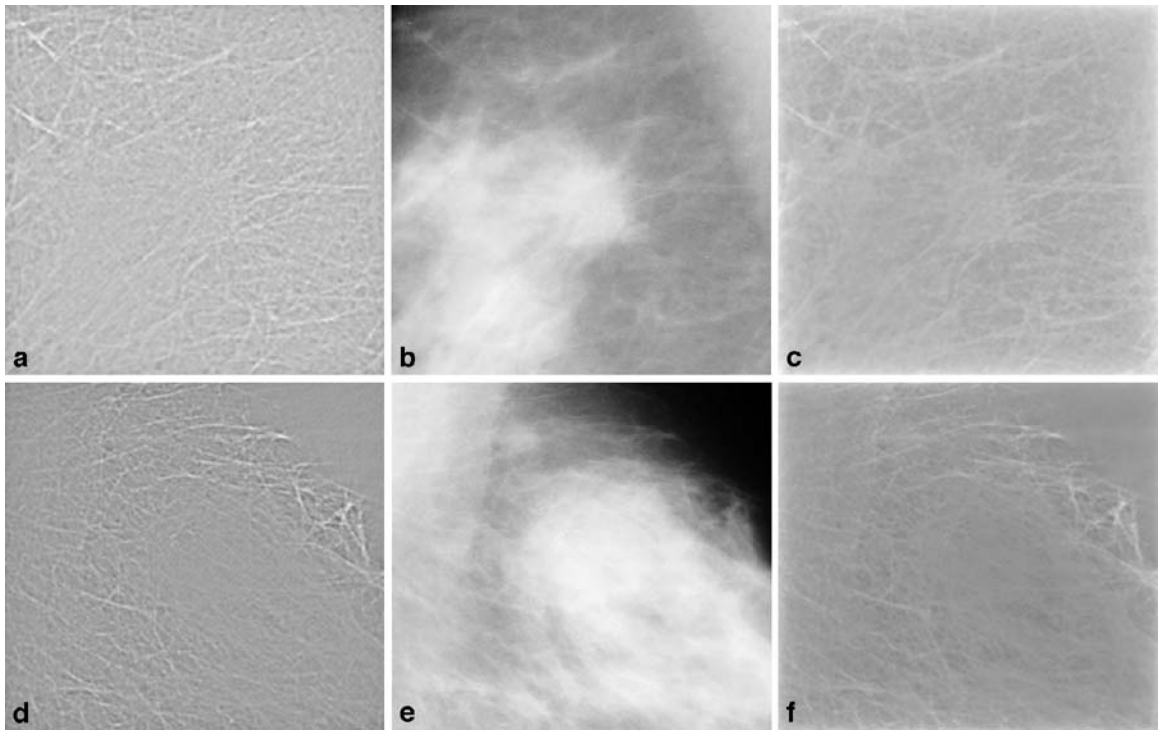

Fig 6. The only two images where most of the readers preferred the images (a, d) enhanced with the DRT-based method than those (c, f) enhanced with the FSS-based method. These were also the only two images where the radiologist found the enhanced images created with the DRT-based method more visually appealing.

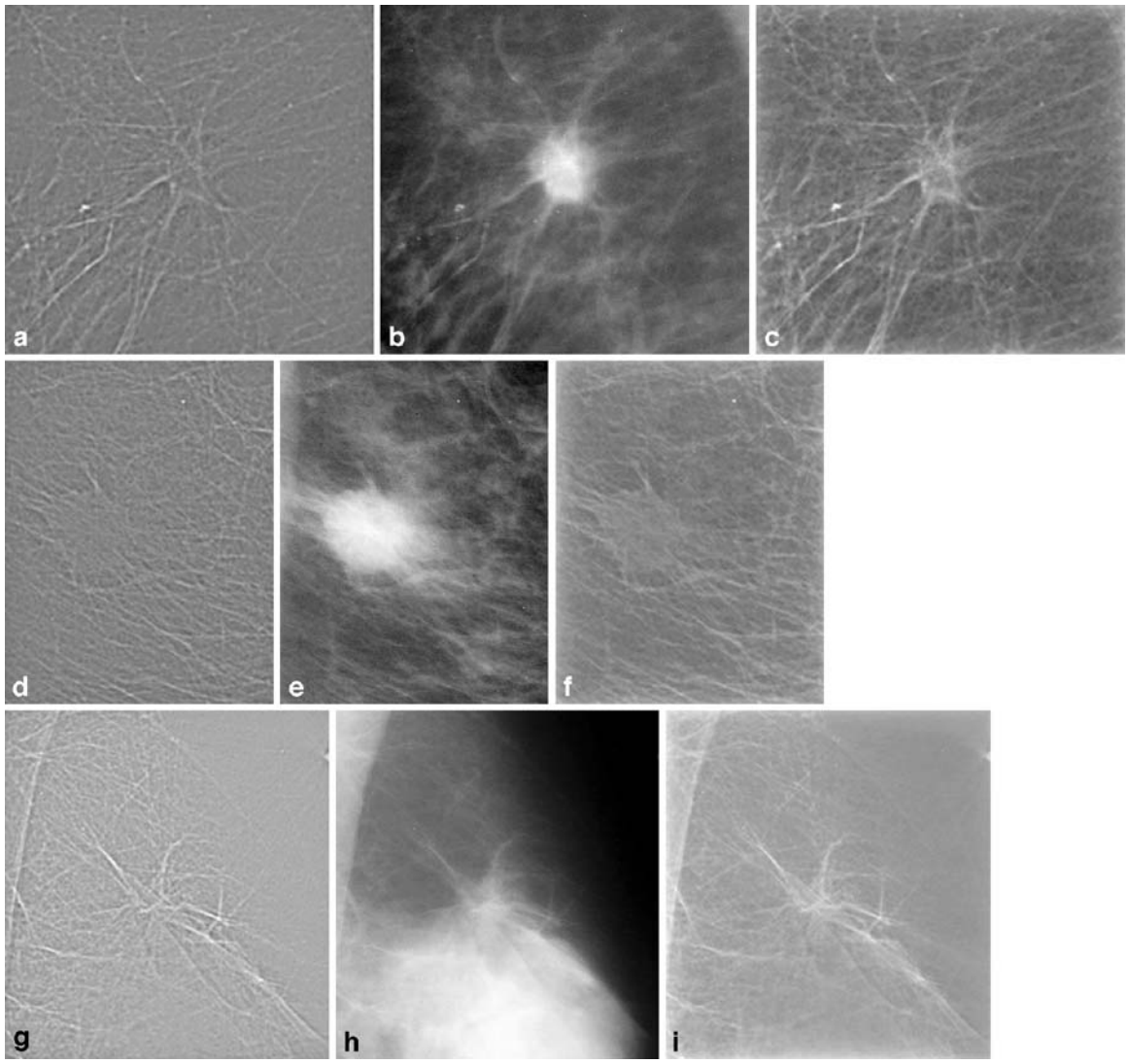

Fig 7. Three images where most of the readers preferred the images (c, f, i) enhanced with the FSS-based method than those (a, d, g) enhanced with the DRT-based method.

In future work, additional observer studies could be conducted to analyze the effect of the enhancement algorithms on detection performance. One could assess if the enhancement techniques help observers to detect more spiculated lesions. The effect of the enhancement methods on CADe algorithms could also be studied. The initial evaluation of CADe algorithms is typically in terms of FROC curves[3] of the algorithms acting independently (i.e., no human observer). However, as CADe algorithms are ultimately used to assist radiologists, confirmatory studies of the performance of the radiologist with and without the use of CADe would also be needed.

CONCLUSION

In this study, we compared the enhanced images obtained with two methods using 2 AFC observer studies. Observers with and without experience in breast imaging were used in these studies and we found that both groups found the images enhanced with the FSS-based method to be more visually

appealing. Thus, by incorporating the FSS-based method (which is a new formulation to compute a DRT) we have been able to improve the performance of our enhancement algorithm. We plan to further evaluate the enhancement algorithms by conducting observer studies to analyze the effect of the enhancement algorihtms on detection performance.

ACKNOWLEDGEMENTS

Mehul P. Sampat was supported by predoctoral fellowship W81XWH-04-1-0406 from the Department of Defense Congressionally Directed Medical Research Program. We thank the University of Texas Center for Biomedical Engineering for seed grant funding. This work was also supported in part by a grant from the Wallace H. Coulter Foundation. We thank the 10 engineering student observers for their participation in this study. Finally, we appreciate the technical support in the Biomedical Informatics Laboratory provided by Chris Kite, Zack Mahdavi, and Scott Swanson. We would also like to thank the anonymous reviewer for his comments, which helped to improve the clarity of the paper.

REFERENCES

1. American Cancer Society: Cancer Facts and Figures 2006. Atlanta: American Cancer Society, 2006

2. Liberman L, Abramson AF, Squires FB, Glassman JR, Morris EA, Dershaw DD: The breast imaging reporting and data system: positive predictive value of mammographic features and final assessment categories. AJR Am J Roentgenol 171:35–40, 1998

3. Sampat MP, Markey MK, Bovik AC: Computer-aided detection and diagnosis in mammography. In: Bovik AC Ed. Handbook of Image and Video Processing, 2nd edition. New York: Academic Press, 2005, pp 1195–1217

4. Giger ML: Computer-aided diagnosis of breast lesions in medical images. Comput Sci Eng 2:39–45, 2000

5. Giger ML, Karssemeijer N, Armato SG, III: Computer-aided diagnosis in medical imaging. IEEE Trans Med Imaging 20:1205–1208, 2001

6. Doi K, MacMahon H, Katsuragawa S, Nishikawa RM, Jiang Y: Computer-aided diagnosis in radiology: potential and pitfalls. Eur J Radiol 31:97–109, 1999

7. Vyborny CJ, Giger ML, Nishikawa RM: Computer-aided detection and diagnosis of breast cancer. Radiol Clin North Am 38:725–740, 2000

8. Vyborny CJ, Doi T, O'Shaughnessy KF, Romsdahl HM, Schneider AC, Stein AA: Breast cancer: importance of spiculation in computer-aided detection. Radiology 215: 703–707, 2000

9. Sampat MP, Whitman GJ, Markey MK, Bovik AC: Evidence-based detection of spiculated masses and architectural distortions. Med Imaging 2005 Image Process 5747: 26–37, 2005

10. Sampat MP, Whitman GJ, Stephens TW, et al: The reliability of measuring physical characteristics of spiculated masses on mammography. Br J Radiol 79:S134–140S, 2006

11. Deans SR: The radon transform and some of its applications. Melbourne: Krieger Publishing, 1983

12. Bracewell RN: Two-dimensional imaging. Englewood Cliffs: Prentice Hall, 1995

13. Kelley BT, Madisetti VK: The fast discrete radon transform. I. Theory. IEEE Trans Image Process 2:382–400, 1993

14. Gotz WA, Druckmuller HJ: A fast digital radon transform—an efficient means for evaluating the Hough transform. Pattern Recognit 29:1985–1992, 1995

15. Matej S, Fessler JA, Kazantsev IG: Iterative tomographic image reconstruction using Fourier-based forward and back-projectors. IEEE Trans Med Imaging 23:401–412, 2004

16. Basu S, Bresler Y: O(N2log2N) filtered backprojection reconstruction algorithm for tomography. IEEE Trans Image Process 9:1760–1773, 2000

17. Elbakri IA, Fessler JA: Statistical image reconstruction for polyenergetic X-ray computed tomography. IEEE Trans Med Imaging 21:89–99, 2002

18. Zeng GL: Image reconstruction—a tutorial. Comput Med Imaging Graph 25, 2001

19. Heath M, Bowyer KW, Kopans D, Moore R, Kegelmeyer P, Jr: The digital database for screening mammography. In: 5th International Workshop on Digital Mammography. Toronto, Canada, 2000

20. Averbuch A, Coifman RR, Donoho DL, Israeli M, Walden J: Fast Slant Stack: A notion of radon transform for Data in a Cartesian Grid which is rapidly computible, algebraically exact, geometrically faithful and invertible. http://www.stat.stanford.edu/~donoho/reports.html, in press